Spontaneous parametric down-conversion in a three-level system

Jianming Wen,[1] Shengwang Du,[2] and Morton H. Rubin[1]
[1]*Physics Department, University of Maryland, Baltimore County, Baltimore, Maryland 21250, USA*
[2]*Edward L. Ginzton Laboratory, Stanford University, Stanford, California 94305, USA*
(Received 30 April 2007; published 20 July 2007)

We have studied the space-time entangled Stokes-anti-Stokes photons generated from a three-level system. In the presence of counterpropagating pump and control lasers, paired Stokes and anti-Stokes fields are spontaneously emitted into opposite directions. The two-photon wave packet is generally a convolution of the phase matching and the third-order nonlinear susceptibility and the feature of the joint temporal correlation is determined by either of them. When the phase matching plays a major role in determining the spectral width of biphotons, the two-photon interference exhibits as conventional type-II spontaneous parametric down-conversion (SPDC). However, if the spectral width of paired photons is determined by the third-order nonlinear susceptibility, two types of four-wave mixings (FWMs) destructively interfere and contribute to the two-photon coincidences. In such a case, the coincidence counting rate appears as a damped Rabi oscillation and exhibits the photon antibunching. The oscillation frequency is equal to the effective Rabi frequency. We have also discussed polarization-entanglement generation in a three-state case. It is found that if the phase matching is crucial in determining the properties of paired Stokes and anti-Stokes photons, the generated state is the same as the degenerate type-II SPDC. However, if the spectral width is mainly controlled by the resonant linewidths in the third-order nonlinearity, one can select one FWM to produce polarization-entangled biphotons, but paired photons from the other FWM process is nonpolarization entangled.

DOI: 10.1103/PhysRevA.76.013825 PACS number(s): 42.65.Lm, 42.50.Dv, 42.65.An, 32.80.−t

I. INTRODUCTION

Paired photons occupy an important place in quantum optics, since they have offered quantum optics with one of its most powerful tools to explore phenomena such as particle entanglement and the idea of information teleportation, providing potential applications to quantum information processing [1]. In addition, paired photons have become a powerful means to test the interpretation of quantum theory [2–5]. Many exciting research fields based on entangled photons have emerged and besides the applications mentioned above, they also include quantum imaging [6], quantum lithography [7], and quantum optical measurement [8].

It has been known for a long time that there is a tie connection between quantum optics and nonlinear optics, and the process of the nonlinear optical interaction has already been used to produce the entangled photon pairs. One standard technique to generate paired photons is to use the spontaneous parametric down-conversion (SPDC) [9,10], in which a strong pump laser drives the atomic oscillators in a noncentrosymmetric crystal into a nonlinear region, and then two down-converted beams are radiated by these oscillators. The SPDC source has been extensively studied experimentally and theoretically in the last two decades. Recently, a new type of biphoton resource using the electromagnetically induced transparency (EIT) [11] and four-wave mixing (FWM) has attracted much attention in both experiments [12–15] and theories [16–18]. Compared with the conventional SPDC source, this new resource of entangled photons has such benefits as narrow spectral width, high conversion efficiency, long coherence time, and long coherence length. In the photon coincidence counting detection, it may reveal the intrinsic information about the biphoton-generation mechanism from the FWM processes, e.g., the dephasing rate or the decay rate.

Paired Stokes and anti-Stokes photons generated from a double-Λ (four-level) atomic configuration have been theoretically analyzed in [16,18], where optical properties of correlated photons have been examined by both perturbation theory and coupled (Maxwell) field-operator equations. The EIT effect is built into the anti-Stokes channel so that the anti-Stokes photons, resonant with the corresponding atomic transition, can propagate through the medium without almost absorption and along with a small group velocity. The recent study about biphotons emitted via a two-level system [15,17] shows a damped Rabi oscillation and the anti-bunching-like effect in the two-photon coincidence counting measurement, which is due to the destructive interference between two types of FWMs occurring in the medium. It is also pointed out that the nonlinear coupling coefficients for the coupled field-operator equations are different than those for the classical FWM coupled field equations. However, the linear Rayleigh scattering of the pump beam limits the visibility in the second-order quantum coherence function. Using biphotons generated from a two-level system, a new two-photon beating experiment [19] has been recently proposed in the resonant pumping case. It is found that in the resonant pumping case, the linear response to biphotons from each component in the Mollow triplet is different: the central part propagates with unity refractive index while two sidebands propagate with tunable indexes of refraction and vanishing absorption. This refractive-index difference causes the central part of the two-photon temporal correlation to switch from the anti-bunching-like effect to the bunchinglike effect. Twin photons (entangled Stokes and anti-Stokes) produced via a three-level system has been recently studied in the experiment [14]. However, the optical responses (linear and nonlinear susceptibilities) are obtained by replacing the four-level results as the three-level results. In this paper, we present a rigorous method to treat the issues of paired photon generation and

FWM in a three-level double-Λ-configuration system. The dynamics of the atomic ensemble is rigorously derived by adopting the same methodology introduced in [17,20].

Motivated by the work [15,17], in [21] we have studied the FWMs in a three-level system and find that, both the constructive and destructive interference of the third-order nonlinear susceptibility of the conjugate field can be realized by choosing different control-laser detunings. Further, the polarization of the generated conjugate field is also controllable by adjusting the control detuning. In this paper, the detailed analysis on the spontaneous parametric generation is made upon the first-order perturbation theory. An example of a counterpropagation geometry and the backward generation is provided. We find that there are two types of FWM processes contributing to paired Stokes-anti-Stokes generation. In the large pump-beam detuning, since the nonlinearity is very small, it allows us to approximate the output state at the output surface(s) of the material in the two-photon limit by the time-dependent perturbation theory. Besides, the two-photon amplitude is of importance in most of biphoton optics. The feature of the coincidence counting rate is found to be determined by the effects either from the phase matching or from the third-order nonlinearity. The biphoton wave packet is generally a convolution of the phase matching and the third-order nonlinear susceptibility. If the phase matching is dominant in determining the biphoton wave packet, the joint detection probability behaves as the type-II SPDC case. If the paired photon wave packet is mainly governed by the third-order nonlinearity, the probability shows a damped Rabi oscillation due to the destructive interference between two types of FWMs present in the system. The oscillation frequency is equal to the effective Rabi frequency Ω_e, and the damping rate is determined by the resonant linewidths for biphoton generation. The theory agrees with the experimental data [14] in such a case. Another effort is made to generate the polarization-entangled Stokes and anti-Stokes photons in a three-state scheme. It is found that if the phase matching is much more important in determining the biphoton properties, the polarization entanglement is the same as the degenerate type-II SPDC and the information about the two types of paired photons is washed out. However, if the structure of the third-order nonlinearity is crucial, to create the polarization entangled state, one needs the postselection technique by filtering one of FWMs. In this paper, the discussions are concentrated on the two-photon temporal correlation in the counterpropagating geometry. The transverse properties of paired photons can be studied by following the analysis given in [16,22]. For simplicity, in this paper the Doppler effect and Langevin noise operators will not be taken into account.

The paper is organized as follows. In Sec. II, we formulate the optical response of the three-level system in full quantum theory. By adopting the method introduced in [17,20], the first-order linear susceptibility and third-order nonlinear susceptibility are obtained. The linear optical responses to the Stokes and anti-Stokes fields are crucial not only in determining their dispersion profiles and transmission spectrums, but in controlling the spectral width of the biphoton wave packet. The nonlinear susceptibility determines the parametric conversion efficient and also governs the feature

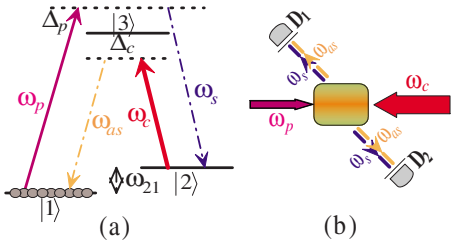

FIG. 1. (Color online) (a) Four-wave mixing and biphoton generation in a three-level system. A weak pump beam with frequency ω_p and detuning Δ_p is applied to the atomic transition $|1\rangle \rightarrow |3\rangle$ and a strong control field with frequency ω_c and detuning Δ_c pumps the transition $|2\rangle \rightarrow |3\rangle$. Paired Stokes and anti-Stokes fields are irradiated at the frequencies $\omega_s = \varpi_s + \delta$ and $\omega_{as} = \varpi_{as} - \delta$, respectively. (b) Schematic of a simplified experimental setup. In the presence of the counterpropagating pump and control beams, paired Stokes and anti-Stokes photons trigger photodetectors D_1 and D_2 in the backward geometry.

of the two-photon amplitude or biphoton wave packet. In Sec. III, using the first-order perturbation theory we obtain the paired Stokes and anti-Stokes wave packet in the Schrödinger picture. The spectral width of biphotons is determined by either the phase matching or the resonant linewidths in the third-order nonlinearity. In Sec. IV, paired Stokes and anti-Stokes photons are studied in both the singles and coincidence counting measurements. Considering the importance of the phase matching and nonlinearity in determining the biphoton wave packet, we divide the two-photon correlation into two regions: phase-matching-determined and nonlinearity-determined. Further, we also analyze the polarization-entangled Stokes and anti-Stokes photons in a three-state scheme. Finally, the Summary is provided.

II. OPTICAL RESPONSE OF A THREE-LEVEL SYSTEM

We begin with a medium of identical three-level atoms or molecules initially prepared in their ground level $|1\rangle$ [see Fig. 1(a)]. The idealized atoms or molecules are confined within a long, thin cylindrical volume with a length L and cross section area A. The averaged atomic density is N. The schematic of an ideal three-level system is a Λ-type atomic configuration shown in Fig. 1(a). A simplified experimental setup for paired photon generation in such a three-level system is illustrated in Fig. 1(b), where a weak pump laser with angular frequency ω_p and a strong control field with angular frequency ω_c are counterpropagating through the medium. Paired Stokes and anti-Stokes photons are spontaneously emitted into opposite directions, as shown in Fig. 1(b). The weak pump beam is applied to the atomic transition $|1\rangle \rightarrow |3\rangle$ with a detuning $\Delta_p = \omega_{31} - \omega_p$; and the strong control laser is tuned to the quantum transition $|2\rangle \rightarrow |3\rangle$ with a detuning $\Delta_c = \omega_{32} - \omega_c$, where $\omega_{ij} = \omega_i - \omega_j$ is the transition frequency from level $|i\rangle$ to level $|j\rangle$. Two ground levels $|1\rangle$ and $|2\rangle$ are metastable, and the energy difference between them is $\hbar\omega_{21}$. The generated Stokes photons have a central frequency of $\varpi_s = \omega_{32} - \Delta_p$ and the correlated anti-Stokes photons have a central frequency of $\varpi_{as} = \omega_{31} - \Delta_c$, as indicated by the

dashed lines in Fig. 1(a). The two-photon detuning is defined as $\Delta_{21}=\omega_{21}-(\omega_p-\omega_c)$ (or $\Delta_{21}=\Delta_p-\Delta_c$). The character of this nonlinear process can be profoundly modified due to the strong intensity of control (and pump) laser and in such a case, perturbation theory is not sufficient to describe the interaction between the material and two input fields. In the photon counting measurements, two photodetectors D_1 and D_2 are arranged in the backward geometry to record the paired Stokes-anti-Stokes photons. If $\mathbf{k}_p+\mathbf{k}_c=0$ is satisfied, one can choose the right-angle experimental setup to eliminate the background noise from Rayleigh scattering of the pump and control fields. (In fact, because of no well-defined phase matching in the backward geometry, the right-angle experimental setup can be chosen even if $\mathbf{k}_p+\mathbf{k}_c\neq 0$.) Here $\mathbf{k}_p$ and $\mathbf{k}_c$ are wave vectors of the pump and control fields. For simplicity, in this paper we will focus on an ideal system in which the Doppler broadening will not be taken into account.

The dynamics of a single atom is characterized by its atomic operators, which at the initial time are defined as

$$Q_{ij}=|i\rangle\langle j| \quad (i,j=1,2,3),$$

and satisfy the Heisenberg operator equation of motion in the dipole approximation

$$\dot{Q}_{mn}=i\omega_{mn}Q_{mn}+i\sum_{\ell}(d_{n\ell}EQ_{m\ell}-d_{\ell m}EQ_{\ell n}). \tag{1}$$

Here the subscripts (m,n,ℓ) run over among (1, 2, 3), E is the total electric field operator and $\mathbf{d}_{n\ell}=\langle n|\mathbf{d}|\ell\rangle/\hbar$ is the dipole matrix element divided by $\hbar$. Considering the arrangements of optical pumping, we write the positive-frequency electric field operators as

$$E_1e^{-i\omega_pt}=e^{-i\omega_pt}[E_p+E_{as}^{(+)}e^{-i(\Delta_{21}+\delta)t}],$$

$$E_2e^{-i\omega_ct}=e^{-i\omega_ct}[E_c+E_s^{(+)}e^{i(\Delta_{21}+\delta)t}], \tag{2}$$

where E_p and E_c represent the slowly varying amplitudes of two classical pump and control fields, and $E_s^{(+)}$ and $E_{as}^{(+)}$ are field operators of generated Stokes and anti-Stokes photons. In Eq. (2), the energy conservation in the process is applied, i.e., $\omega_p+\omega_c-\omega_s-\omega_{as}=0$. To eliminate the fast oscillating phase terms in Eq. (1), we introduce the following transformations:

$$\sigma_{ii}=Q_{ii} \quad (i=1,2,3),$$

$$\sigma_{31}=Q_{31}e^{-i\omega_pt},$$

$$\sigma_{32}=Q_{32}e^{-i\omega_ct},$$

$$\sigma_{21}=Q_{21}e^{-i(\omega_p-\omega_c)t}. \tag{3}$$

Now using Eqs. (1)–(3), one can obtain a set of equations which the atomic evolution obeys as follows:

$$\begin{aligned}
\dot{\sigma}_{11}=&-\gamma_1\sigma_{11}+id_{13}[E_p^*+E_{as}^{(-)}e^{i(\Delta_{21}+\delta)t}]\sigma_{13}\\
&-id_{31}[E_p+E_{as}^{(+)}e^{-i(\Delta_{21}+\delta)t}]\sigma_{31}+\mathcal{F}_{11},\\
\dot{\sigma}_{22}=&-\gamma_2\sigma_{22}+id_{23}[E_c^*+E_s^{(-)}e^{-i(\Delta_{21}+\delta)t}]\sigma_{23}\\
&-id_{32}[E_c+E_s^{(+)}e^{i(\Delta_{21}+\delta)t}]\sigma_{32}+\mathcal{F}_{22},\\
\dot{\sigma}_{33}=&-\gamma_3\sigma_{33}+id_{31}[E_p+E_{as}^{(+)}e^{-i(\Delta_{21}+\delta)t}]\sigma_{31}\\
&-id_{13}[E_p^*+E_{as}^{(-)}e^{i(\Delta_{21}+\delta)t}]\sigma_{13}\\
&+id_{32}[E_c+E_s^{(+)}e^{i(\Delta_{21}+\delta)t}]\sigma_{32}\\
&-id_{23}[E_c^*+E_s^{(-)}e^{-i(\Delta_{21}+\delta)t}]\sigma_{23}+\mathcal{F}_{33},\\
\dot{\sigma}_{31}=&i\Gamma_p\sigma_{31}-id_{13}[E_p^*+E_{as}^{(-)}e^{i(\Delta_{21}+\delta)t}](\sigma_{11}-\sigma_{33})\\
&-id_{23}[E_c^*+E_s^{(-)}e^{-i(\Delta_{21}+\delta)t}]\sigma_{21}+\mathcal{F}_{31},\\
\dot{\sigma}_{32}=&i\Gamma_c\sigma_{32}+id_{23}[E_c^*+E_s^{(-)}e^{-i(\Delta_{21}+\delta)t}](\sigma_{33}-\sigma_{22})\\
&-id_{13}[E_p^*+E_{as}^{(-)}e^{i(\Delta_{21}+\delta)t}]\sigma_{12}+\mathcal{F}_{32},\\
\dot{\sigma}_{21}=&i\Gamma_{21}\sigma_{21}+id_{13}[E_p^*+E_{as}^{(-)}e^{i(\Delta_{21}+\delta)t}]\sigma_{23}\\
&-id_{32}[E_c+E_s^{(+)}e^{i(\Delta_{21}+\delta)t}]\sigma_{31}+\mathcal{F}_{21}.
\end{aligned} \tag{4}$$

In Eq. (4), γ_j $(j=1,2,3)$ are decay rates for each level, $\Gamma_p=\Delta_p+i\gamma_{31}$ is the complex pump detuning with dephasing rate γ_{31} between levels $|3\rangle$ and $|1\rangle$, $\Gamma_c=\Delta_c+i\gamma_{32}$ is the complex control detuning with dephasing rate γ_{32} between $|3\rangle$ and $|2\rangle$, and $\Gamma_{21}=\Delta_{21}+i\gamma_{21}$ is the two-photon complex detuning with dephasing rate γ_{21} between two ground levels. $\mathcal{F}_{\alpha\beta}$ $(\alpha,\beta=1,2,3)$ are the quantum Langevin noise operators. Since these Langevin noise operators [23] introduce the unpaired photons, which are not of interest here, we will ignore them from now on. Without considering the Stokes and anti-Stokes fields, as expected from Eqs. (4) they reduce to a set of equations, which describe the atomic dynamics of a three-level EIT-like system.

In general, Eqs. (4) cannot be readily solved for the fields given in Eq. (2). Instead, we will extend the treatment in [17] to the three-level system and try to find a solution keeping all orders to control field E_c while maintaining the lowest order in E_s (E_{as}) of two weak fields. Therefore, the steady-state solutions of Eqs. (4) are required to be of the form

$$\sigma_{jj}=a_{jj}+b_{jj}e^{-i(\Delta_{21}+\delta)t}+c_{jj}e^{i(\Delta_{21}+\delta)t} \quad (j=1,2,3),$$

$$\sigma_{31}=a_{31}+b_{31}e^{-i(\Delta_{21}+\delta)t}+c_{31}e^{i(\Delta_{21}+\delta)t},$$

$$\sigma_{32}=a_{32}+b_{32}e^{-i(\Delta_{21}+\delta)t}+c_{32}e^{i(\Delta_{21}+\delta)t},$$

$$\sigma_{21}=a_{21}+b_{21}e^{-i(\Delta_{21}+\delta)t}+c_{21}e^{i(\Delta_{21}+\delta)t}. \tag{5}$$

Here a_{mn} $(m,n=1,2,3)$ are the solutions for the case in which only the pump (E_p) and control (E_c) fields are present

in the system, as stated above, while the other terms are assumed to be small such that $|b_{mn}|, |c_{mn}| \ll |a_{mn}|$ are satisfied. Again, the population is assumed to be mostly distributed in the ground level $|1\rangle$, i.e., setting $a_{11} \approx 1$.

We next plug the trial solution (5) into Eqs. (4) and look at the terms with the same time dependence. As mentioned above, we will drop any term that contains the product of more than one small quantity. Then after some algebra, we obtain the following quantities of interest:

$$a_{13} = -\frac{2\Gamma_{21}^* \Omega_p}{|\Omega_c|^2 - 4\Gamma_p^* \Gamma_{21}^*}, \tag{6}$$

$$a_{23} = -\frac{|\Omega_p|^2 \Omega_c}{2\Gamma_c^* (|\Omega_c|^2 - 4\Gamma_p \Gamma_{21})}, \tag{7}$$

$$b_{23} = -\frac{4\Gamma_{21}}{|\Omega_c|^2 - 4\Gamma_p \Gamma_{21}} \frac{(\delta - i\gamma_{21})|\Omega_p|^2 d_{32} E_s^{(+)}}{(\Delta_p + \delta - i\gamma_{32})[|\Omega_c|^2 + 4(\Delta_c - \delta + i\gamma_{31})(\delta - i\gamma_{21})]} - \frac{\Omega_p \Omega_c d_{13} E_{as}^{(-)}}{(\Delta_p + \delta - i\gamma_{32})[|\Omega_c|^2 + 4(\Delta_c - \delta + i\gamma_{31})(\delta - i\gamma_{21})]}, \tag{8}$$

$$c_{13} = -\frac{4(\delta + i\gamma_{21}) d_{31} E_{as}^{(+)}}{|\Omega_c|^2 + 4(\Delta_c - \delta - i\gamma_{31})(\delta + i\gamma_{21})} + \frac{4\Gamma_{21}^*}{|\Omega_c|^2 - 4\Gamma_p^* \Gamma_{21}^*} \frac{\Omega_p \Omega_c d_{23} E_s^{(-)}}{|\Omega_c|^2 + 4(\Delta_c - \delta - i\gamma_{31})(\delta + i\gamma_{21})}, \tag{9}$$

where we have defined $\Omega_p = 2d_{31}E_p$ as the pump Rabi frequency and $\Omega_c = 2d_{32}E_c$ as the control Rabi frequency. In the derivation of Eqs. (6) and (9), we have assumed that $|\Delta_p|$ is the dominant quantity and most of the population is located at the ground level (i.e., $a_{11} = 1$). The physics of Eqs. (6) and (9) can be understood as follows. Equations (6) and (7) describe the optical responses of the medium to the pump and control lasers, respectively. When the control field is tuned resonantly with the atomic transition $|2\rangle \rightarrow |3\rangle$, these two equations reduce to the standard EIT result, as expected. It can be seen that the absorption to the pump beam is small and its propagation is associated with a small group velocity [see Eq. (6)]. Similarly, the absorption to the control field is also small, as indicated in Eq. (7). Equations (8) and (9) give the optical responses to the generated Stokes and anti-Stokes fields, respectively. As we will see below, among those terms two contribute to the linear susceptibilities and the other two to the third-order nonlinear susceptibilities, which are the quantities of interest in the photon pairs generation. On the right-hand side (RHS) of Eq. (8), the first term corresponds to the linear response to the generated Stokes photons and the second term to the generation of correlated photon pairs. In addition, the linear response to the Stokes field is manipulated by the EIT-like effect and Raman gain. Similarly, on the RHS of Eq. (9), the first term gives the information of the linear optical response to the anti-Stokes field while the second term is related to the third-order nonlinear susceptibility. As one can see, the linear response has an EIT-like form and the nonlinear part possesses two EIT-like effects, in which one is between the pump and control.

One may notice that the nonlinear response to the anti-Stokes field is somewhat different than that to the Stokes field. However, to fulfill the assumption about the ground-level population being almost unity, it requires $|\Delta_p| \gg |\Omega_{p,c}|$. Under such a situation, Eqs. (8) and (9) become

$$b_{23} = \frac{|\Omega_p|^2}{|\Gamma_p|^2} \frac{(\delta - i\gamma_{21}) d_{32} E_s^{(+)}}{D^*(\delta)} - \frac{\Omega_p \Omega_c d_{13} E_{as}^{(-)}}{(\Delta_p - i\gamma_{32}) D^*(\delta)}, \tag{10}$$

$$c_{13} = -\frac{(\delta + i\gamma_{21}) d_{31} E_{as}^{(+)}}{D(\delta)} - \frac{\Omega_p \Omega_c d_{23} E_s^{(-)}}{(\Delta_p - i\gamma_{32}) D(\delta)}, \tag{11}$$

where

$$D(\delta) = |\Omega_c|^2 + 4(\Delta_c - \delta - i\gamma_{31})(\delta + i\gamma_{21}). \tag{12}$$

Again, in deriving Eqs. (10) and (11) we have required the pump detuning Δ_p being the most dominant quantity. The physics behind Eqs. (10) and (11) now is much clearer: (1) the linear responses to the Stokes and anti-Stokes fields take the form of EIT-like expressions, the anti-Stokes field crosses through the medium along with the (EIT) absorption, and the Stokes field experiences the Raman gain; and (2) the third-order nonlinearities to ω_s and ω_{as} have the same format. The contribution from the Raman gain is small compared to the (EIT) absorption, as long as the assumption that the majority of the population is in the ground level is satisfied. One interesting phenomenon appears when one designs a FWM experiment by applying the linearly polarized pump and control fields working in the degenerate case, i.e., the input probe (Stokes or anti-Stokes) beam has the same central frequency as the generated conjugate field $\varpi_s = \varpi_{as}$. This degenerate situation can be achieved by satisfying the equality $\omega_{21} = -\Delta_p \pm \Omega_e$, where Ω_e is the effective Rabi frequency as defined in the following. In such an experimental arrangement, there is an interference occurring between two types of FWMs due to possible transition pathways, as discussed in [21]. Another interesting thing appears when the scheme is chosen to manipulate the polarization of the generated (conjugate) field in the three-state system. It is found that the polarization of the generated beam is controllable by adjusting the coupling detuning Δ_c. A detailed analysis shows that

the conjugate field may alter from the linear polarization to the circular polarization (for details, see [21]). Third, when $\omega_{21}=-\Delta_p\pm\Omega_e$ is established, in the regime of spontaneous emission the scheme can be used to produce polarization-entangled photon pairs, which possess many potential applications such as tests of Bell's inequalities [24] and quantum cryptography [25]. The generation of polarization entanglement will be further discussed in Sec. IV C.

In addition, the second term on the RHS of Eq. (11) shows a resonance whenever the pump beam is tuned to the line center so that $\Delta_p=0$, or whenever the real part of the function $D(\delta)$ gives a zero. In the limit $\Delta_c\to 0$, i.e., the case of the control field resonant with transition $|2\rangle\leftrightarrow|3\rangle$, the zeros of $D(\delta)$ occur near $\delta=\pm\frac{|\Omega_c|}{2}$. In general, the control beam is not exactly resonant with the atomic transition and the full form of Eq. (12) should be kept. Solving $\mathrm{Re}[D(\delta)]=0$, a doublet of resonances appears at

$$\delta_\pm=\frac{\Delta_c\pm\sqrt{\Omega_e^2+4\gamma_{31}\gamma_{21}}}{2}, \tag{13}$$

where we have introduced the effective Rabi frequency $\Omega_e=\sqrt{\Delta_c^2+|\Omega_c|^2}$. To further understand the physical process behind $D(\delta)$, we assume $\Omega_e\gg(\gamma_{31},\gamma_{21})$. Under such an assumption, the doublet resonances occur at $\delta_\pm=(\Delta_c\pm\Omega_e)/2$ and they are well separated. Near the resonance at $\delta_-=(\Delta_c-\Omega_e)/2$, $D(\delta)$ can be approximated as

$$D(\delta)=4\Omega_e(\delta-\delta_-+i\Gamma_-),\quad \Gamma_-=\frac{\gamma_{31}+\gamma_{21}}{2}+\frac{\Delta_c}{\Omega_e}\frac{\gamma_{21}-\gamma_{31}}{2}. \tag{14}$$

Γ_- represents the linewidth of this resonance. In the case of $\Delta_c\to 0$, Γ_- goes to $\frac{\gamma_{31}+\gamma_{21}}{2}$ while in the case of large control detuning, i.e., $|\Delta_c|\gg|\Omega_c|$, Γ_- approaches γ_{21}. In the same way, near the resonance at $\delta_+=(\Delta_c+\Omega_e)/2$, $D(\delta)$ can be approximated as

$$D(\delta)=-4\Omega_e(\delta-\delta_++i\Gamma_+),\quad \Gamma_+=\frac{\gamma_{31}+\gamma_{21}}{2}+\frac{\Delta_c}{\Omega_e}\frac{\gamma_{31}-\gamma_{21}}{2}. \tag{15}$$

As seen from Eq. (15), Γ_+ also goes to $\frac{\gamma_{31}+\gamma_{21}}{2}$ as the control is near resonant with the transition; while it reaches γ_{31} as $|\Delta_c|\gg|\Omega_c|$. Two types of FWMs appear behind $D(\delta)$. One FWM process happens when the central frequency of the anti-Stokes field is $\varpi_{as}=\omega_{31}-\delta_+$ and the central frequency of the Stokes field is $\varpi_s=\omega_{32}-\Delta_p-\delta_-$. The other FWM occurs as the anti-Stokes field is peaked at $\varpi_{as}=\omega_{31}-\delta_-$ while the Stokes field peaks at $\varpi_s=\omega_{32}-\Delta_p-\delta_+$. As expected, both FWMs satisfy the energy conservation $\omega_p+\omega_c-\varpi_{as}-\varpi_s=0$.

In the following discussions, we focus on the large pump-detuning case. Let us look at the optical response of the atomic dipoles at frequencies $\varpi_s+\delta$ and $\varpi_{as}-\delta$. The slowly varying amplitudes of polarization operators for a medium are given by $\mathcal{P}_s(-\delta)=N\hbar d_{23}b_{23}$ and $\mathcal{P}_{as}(\delta)=N\hbar d_{13}c_{13}$ with the atomic density N. It is known that the relationship between the polarization and the susceptibility is $\mathcal{P}=\varepsilon_0\chi E+\varepsilon_0\chi^{(3)}EEE$, where χ is the effective linear susceptibility and $\chi^{(3)}$ is the third-order nonlinear susceptibility. Utilizing Eqs. (10) and (11), one can obtain

$$\chi_s(-\delta)=\frac{N\hbar|d_{32}|^2|\Omega_p|^2(\delta-i\gamma_{21})}{\varepsilon_0|\Gamma_p|^2D^*(\delta)}, \tag{16}$$

$$\chi_{as}(\delta)=-\frac{N\hbar|d_{31}|^2(\delta+i\gamma_{21})}{\varepsilon_0 D(\delta)}, \tag{17}$$

$$\chi_s^{(3)}(-\delta)=-\frac{4N\hbar|d_{13}d_{23}|^2}{\varepsilon_0(\Delta_p-i\gamma_{32})D^*(\delta)}, \tag{18}$$

$$\chi_{as}^{(3)}(\delta)=-\frac{4N\hbar|d_{23}d_{13}|^2}{\varepsilon_0(\Delta_p-i\gamma_{32})D(\delta)}. \tag{19}$$

The linear susceptibilities $\chi_s(-\delta)$ and $\chi_{as}(\delta)$ determine the dispersion profile and transmission spectrum of the generated Stokes and anti-Stokes fields passing through the medium, respectively. In general, the natural spectral width of photon pairs is controlled by the phase dispersion, which is dependent on the linear susceptibility as shall be discussed below. The third-order nonlinear susceptibilities $\chi_s^{(3)}(-\delta)$ and $\chi_{as}^{(3)}(\delta)$ will govern the parametric conversion efficiency of twin beams, and meanwhile they play an important role in the two-photon amplitude (or biphoton wave packet). For example, the integration over the full frequency spectrum will yield the two-photon spectral width around the residues [15,17]. Comparing this width with that from the phase dispersion, a narrower one will play a major role in the biphoton wave packet. Equations (16)–(19) have also included the effect of power broadening. It is useful to look at the features of these optical responses. In Fig. 2, we have plotted the linear and nonlinear optical responses to the anti-Stokes field. The first-order susceptibility to the anti-Stokes beam is depicted in Fig. 2(a), where the blue solid line describes the real part and the red point line is the imaginary part. The third-order nonlinear susceptibility is shown in Fig. 2(b). As seen from Fig. 2(b), in the spectrum of paired photon generation, there are doublet resonances, which indicate two types of FWMs discussed above. The doublet resonances are separated by the effective Rabi frequency Ω_e. The linear responses to these doublets behave as a two-level system [see Fig. 2(a)]. The slopes of the real part of the linear susceptibility determine the group velocity while the imaginary part controls the transmission profile.

Before proceeding with the discussion, let us look at the phase matching of the FWM processes in a three-level system. The propagation constants of two weak fields within the medium are given by $k_{as}=(\varpi_{as}+\delta)/v_{as}$ and $k_s=(\varpi_s-\delta)/v_s$, respectively. v_s and v_{as} are group velocities of Stokes and anti-Stokes photons propagating through the system, which are defined by $v=c/[n+\omega(dn/d\omega)]$. $n(\omega)$ is the refractive index experienced by each weak field and is defined as $n=\sqrt{1+\mathrm{Re}[\chi]}$, where $\mathrm{Re}[x]$ stands for choosing the real part of the quantity x. It is found that only when the coupling laser is (near) resonant, i.e., $\Delta_c\to 0$, the group velocity of the anti-Stokes field will be dramatically changed because of the EIT effect. Otherwise, its group velocity can be set as the speed

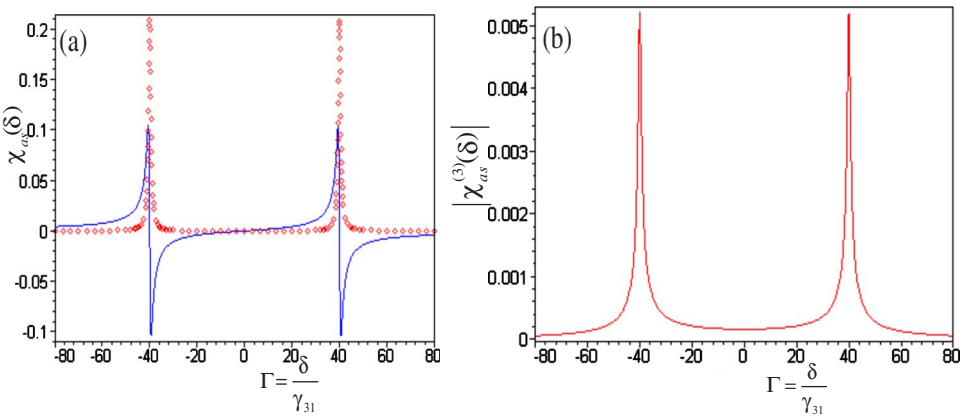

FIG. 2. (Color online) (a) The linear optical response $\chi_{as}(\delta)$ to the anti-Stokes field: the blue solid line represents the real part of the linear susceptibility and the red point line is the imaginary part. (b) The doublet resonances shown in the third-order nonlinear susceptibility $|\chi_{as}^{(3)}(\delta)|$ of the anti-Stokes beam.

of light in the vacuum c. For the Stokes field, its group velocity approaches c because of $|\Omega_p/\Gamma_p| \ll 1$. Therefore, the group velocity of the anti-Stokes field is

$$v_{as} = \frac{c}{1 + \frac{\omega_{31}}{2}\frac{d\,\mathrm{Re}[\chi_{as}(\delta)]}{d\delta}} = \frac{c}{1 + \frac{N\hbar|d_{31}|^2\omega_{31}}{2\varepsilon_0|\Omega_c|^2}}, \quad (20)$$

as the monochromatic control field is tuned near resonantly with its quantum transition. In the counterpropagating geometry, the resulting wave-number mismatch is

$$\Delta k = k_p - k_c + k_{as} - k_s = \left(\frac{1}{v_{as}} + \frac{1}{c}\right)\delta + \frac{2\omega_{21}}{c}, \quad (21)$$

where $k_{p,c} = \omega_{p,c}/c$, $k_s = (\varpi_s - \delta)/c$, and $k_{as} = \varpi_{as}/c + \delta/v_{as}$. The bandwidth due to the group delay can then be estimated as $\Delta\omega_\Phi \sim \frac{cv_{as}}{(c+v_{as})L}$. One special case comes about if $k_p = k_c$. In such a case, paired Stokes and anti-Stokes photons are radiated into the whole 4π space. However, if $k_p \neq k_c$ the generated Stokes and anti-Stokes photons have the directionality and the emitted cones are aligned by the phase mismatching between the pump and control fields, even though the total phase mismatching for FMW is the same as given in Eq. (21). On the other hand, the propagations of the Stokes and anti-Stokes beams are limited by the transmission spectral widths. It is known that the transmission spectral width is determined by the imaginary part of the linear susceptibility χ. Considering the situations here, the transmission profile plays the role only as the control field is near resonant with its transition. In such a case, the anti-Stokes transmission will be controlled by the EIT transparency window. From the expression for the transmission $T(\delta) = e^{-\mathrm{Im}[\chi]kL}$, one can obtain the transmission bandwidth, which is given by

$$\Delta\omega_{tr} = \sqrt{\frac{c}{\varpi_{as}L}\frac{d^2\,\mathrm{Im}[\chi_{as}(\delta)]}{d\delta^2}} = \sqrt{\frac{\epsilon_0 c|\Omega_c|^4}{8N\hbar|d_{31}|^2\omega_{31}L(\gamma_{31}+2\gamma_{21})}}, \quad (22)$$

where $\mathrm{Im}[x]$ means choosing the imaginary part of the quantity x. Again, Eq. (17) has been used in deriving Eq. (22). Including the linear absorption (or gain) into the phase mismatching, we can extend Eq. (21) as [26]

$$\Delta k = \left(\frac{1}{v_{as}} + \frac{1}{c}\right)\delta + \frac{2\omega_{21}}{c} + i\frac{\mathrm{Im}[\chi_{as}]\varpi_{as} + \mathrm{Im}[\chi_s]\varpi_s}{c}. \quad (23)$$

It should be noted that the above result is only valid in the low-gain regime.

Let us look at an example. Consider the ^{87}Rb $D2$ line transition and the parameters are chosen as: $L=2$ cm, $N=2\times10^{17}$ atoms/m^3, $\gamma_{31}=\gamma_{32}=2\pi\times3$ MHz, $\Delta_{21}=2\pi\times480$ MHz, $\omega_{31}=2\pi\times380$ THz, $\gamma_{21}=2\pi\times0.6$ MHz, $|\Omega_p|=80\gamma_{31}$, and $|\Omega_c|=80\gamma_{31}$. The control laser is tuned resonant with its atomic-transition channel. The spectral width resulting from the phase mismatching is at least $\Delta\omega_\Phi \sim 2\pi\times91.5$ MHz and from the transmission profile is $\Delta\omega_{tr} \sim 2\pi\times315$ MHz. By comparing with the linewidths of resonances for paired Stokes and anti-Stokes photons, the biphoton bandwidth is almost determined by the linewidths instead of either the phase dispersion or the transmission profiles. Two resonances are separated around $80\gamma_{31} \simeq 2\pi\times240$ MHz and are inside the transmission spectrum.

III. BIPHOTON WAVE PACKET IN A THREE-LEVEL SYSTEM

Following the treatment used in [9,16], in this section we formulate the biphoton wave packet in a three-level system by perturbation theory. In the interaction picture the effective Hamiltonian is given by

$$\mathcal{H}_I = \epsilon\int_V d^3r\chi_{as}^{(3)}(\delta)E_pE_cE_s^{(-)}E_{as}^{(-)} + \mathrm{H.c.}, \quad (24)$$

where V is the interaction volume illuminated by the pump and control beams together and H.c. stands for the Hermitian conjugate. The generated Stokes and anti-Stokes photons are given by the quantized fields

$$E_j^{(+)} = \sum_{\mathbf{k}_j} E_j a_{\mathbf{k}_j} e^{i(\mathbf{k}_j\cdot\mathbf{r}-\omega_j t)} \quad (j=s,as), \quad (25)$$

where $E_j = i\sqrt{\hbar\omega_j/2\epsilon_0 n_j^2 V_q}$ with the refraction index n_j and the quantization volume V_q. The wave vectors $\mathbf{k}_j$ are evaluated inside the material and $a_{\mathbf{k}_j}$ are the annihilation operators at the output surface associated with $\mathbf{k}_j$. To simplify the calculations, the pump and control beams are taken as the clas-

sical plane waves. In the Hamiltonian (24) we have made the rotating-wave approximation and neglected the reflections from the medium surfaces.

Considering the weak nonlinear interaction, we can obtain the initial state of paired Stokes-anti-Stokes photons by the first-order perturbation theory in the interaction picture. The calculation of the state vector to first order in perturbation theory gives

$$|\Psi\rangle = |0\rangle - \frac{i}{\hbar}\int_{\infty} dt\mathcal{H}_I|0\rangle = |0\rangle + \sum_{\mathbf{k}_s}\sum_{\mathbf{k}_{as}} F(\mathbf{k}_s,\mathbf{k}_{as})a^{\dagger}_{\mathbf{k}_s}a^{\dagger}_{\mathbf{k}_{as}}|0\rangle. \tag{26}$$

As seen in Eq. (26), $|\Psi\rangle$ is a superposition of the vacuum state $|0\rangle$ and states with many numbers of pairs of photons. When the nonlinearity is very small, the second term on the RHS of Eq. (26) approximately reduces to the biphoton state. Since the vacuum state is not interesting here, we ignore the first term in $|\Psi\rangle$ and only keep the second one. So, the two-photon state reads

$$|\Psi\rangle = \sum_{\mathbf{k}_s}\sum_{\mathbf{k}_{as}} F(\mathbf{k}_s,\mathbf{k}_{as})a^{\dagger}_{\mathbf{k}_s}a^{\dagger}_{\mathbf{k}_{as}}|0\rangle. \tag{27}$$

$F(\mathbf{k}_s,\mathbf{k}_{as})$ is called the two-photon spectral function and it takes the form

$$F(\mathbf{k}_s,\mathbf{k}_{as}) = \beta\delta(\omega_p+\omega_c-\omega_s-\omega_{as})\Phi(\Delta kL)H_{tr}(\alpha_{\mathbf{s}},\alpha_{\mathbf{as}},\rho). \tag{28}$$

In Eq. (28), the Dirac δ function comes from the time integral and states the energy conservation. β is a constant, $\beta = i\pi\sqrt{\varpi_s\varpi_{as}}\chi^{(3)}_{as}E_pE_c$. $\Phi(\Delta kL)$ is the longitudinal detuning function, which is the z integral from $-L$ to 0 over the length of the medium

$$\Phi(\Delta kL) = \frac{1-e^{i\Delta kL}}{i\Delta kL}, \tag{29}$$

where $\Delta k = k_p - k_c + k_{as} - k_s$ is the (complex) phase mismatching along the longitudinal axis and given in Eq. (21) [or Eq. (23)]. $H_{tr}(\alpha_{\mathbf{s}},\alpha_{\mathbf{as}},\rho)$ is called the transverse detuning function, which is the integral over the area A of intersection of the beam cross section

$$H_{tr}(\alpha_{\mathbf{s}},\alpha_{\mathbf{as}},\rho) = \frac{1}{A}\int_A d^2\rho e^{-i(\alpha_{\mathbf{s}}+\alpha_{\mathbf{as}})\cdot\rho}. \tag{30}$$

In Eq. (30) we have assumed that A is independent of z. $\alpha_{\mathbf{s}}$ and $\alpha_{\mathbf{as}}$ are transverse wave vectors of Stokes and anti-Stokes photons, respectively. ρ is in the transverse plane normal to the longitudinal axis z. In the limit of a medium with infinite length and cross area, Φ and H_{tr} both become δ functions. Combining with the energy-conservation δ function, they together form perfect phase matching conditions: $\omega_p+\omega_c-\omega_{as}-\omega_s=0$ and $\mathbf{k}_p+\mathbf{k}_c+\mathbf{k}_s+\mathbf{k}_{as}=0$. The natural spectral width of the biphoton wave packet is determined by the longitudinal detuning function Φ. However, as discussed above the linewidths of generated fields also govern the range of bandwidth of the two-photon state. As the example given in Sec. II, the spectral width of paired Stokes-anti-Stokes is mainly determined by the resonance linewidths for two FWMs. In such a case, the longitudinal detuning function is close to unity and the properties of biphotons are mainly determined by the third-order nonlinear susceptibility $\chi^{(3)}$. In the two-photon coincidence counting measurement, the correlation will reveal the feature of $\chi^{(3)}$ as we shall see in the next section.

To simplify the following discussions, we assume that the intersection between the pump and control beams is constant and large enough such that the transverse detuning function (30) is approximated as a δ function. In addition, in this paper we are interested in the two-photon temporal correlation and the wave vectors are replaced by the wave numbers. The transverse effects in paired Stokes and anti-Stokes photons can be analyzed by following the procedure introduced in [16,22].

IV. PHOTON COUNTING MEASUREMENT

To study the optical properties of biphotons produced from a three-level system, we begin with a simple experiment of photon detection measurement, as shown in Fig. 1(b). In the counterpropagating geometry, paired photons are spontaneously emitted and recorded by detectors D_1 and D_2. If $\mathbf{k}_p+\mathbf{k}_c=0$, the generated Stokes and anti-Stokes photons can trigger both detectors and the right-angle experimental setup can be used to eliminate the Rayleigh-scattering background. The joint detection will exhibit a symmetric distribution. In general, $\mathbf{k}_p+\mathbf{k}_c\neq 0$ and this results in the directionality of generated Stokes and anti-Stokes photons. As a consequence, the two-photon correlation is guided by this phase mismatching. Without loss of generality, we assume that the Stokes photons fire detector D_2 while the anti-Stokes photons go to detector D_1.

A. Single-photon detection

First, let us look at the single-photon detection. To study the singles properties of the radiation, we consider an experiment like that depicted in Fig. 1(b) with detector D_2 removed. The average photon counting rate is given by

$$R_{as} = \lim_{T\to\infty}\frac{1}{T}\int_0^T dt_1\langle\Psi|E_1^{(-)}E_1^{(+)}|\Psi\rangle, \tag{31}$$

where the free-space electromagnetic field $E_1^{(+)}$ is defined in analogy with Eq. (25) and it is evaluated at detector D_1's coordinates, spatial position r_1 and trigger time t_1. For simplicity, the detector efficiency is assumed to be 100%.

The second-order field correlation function in Eq. (31) may be written as

$$\langle\Psi|E_1^{(-)}E_1^{(+)}|\Psi\rangle = \sum_{\mathbf{k}}|\langle 0|a_{\mathbf{k}}E_1^{(+)}|\Psi\rangle|^2. \tag{32}$$

Using Eq. (27), from Eq. (32) one can obtain

$$\langle 0|a_{\mathbf{k}}E_1^{(+)}|\Psi\rangle = \sum_{\mathbf{k}_1}\sum_{\mathbf{k}_s}\sum_{\mathbf{k}_{as}} e^{-i\omega_1\tau_1}F(\mathbf{k}_s,\mathbf{k}_{as})\delta_{\mathbf{k}_s,\mathbf{k}}\delta_{\mathbf{k}_{as},\mathbf{k}_1}, \tag{33}$$

where $\tau_1 = t_1 - r_1/c$. Substituting Eq. (33) into Eq. (32) gives

$$\langle \Psi | E_1^{(-)} E_1^{(+)} | \Psi \rangle = \sum_{\mathbf{k}} \left| \sum_{\mathbf{k}_{as}} e^{-i\omega_{as}\tau_1} F(\mathbf{k}, \mathbf{k}_{as}) \right|^2. \quad (34)$$

To further simplify the calculation, we treat the transverse detuning function (30) as a δ function so that the wave vectors can be replaced by wave numbers. To evaluate the Dirac δ function in $F(\mathbf{k}, \mathbf{k}_{as})$, a summation over a wave number is converted into an angular frequency integral

$$\sum_{k_j} \rightarrow \frac{V_Q^{1/3}}{2\pi} \int d\omega_j \frac{dk_j}{d\omega_j} = \frac{V_Q^{1/3}}{2\pi} \int \frac{d\omega_j}{v_j}. \quad (35)$$

The single-photon counting rate hence becomes

$$R_{as} = R_0 \int d\delta |\chi_{as}^{(3)}(\delta) \Phi(\Delta k L)|^2, \quad (36)$$

where all the slowly varying terms and constants are absorbed into R_0. It is obvious that the singles counting rate has no structure on time, as expected.

B. Two-photon coincidence detection

Next, we concentrate on the two-photon temporal correlation, which is the quantity of primary interest. To study the optical properties of paired Stokes and anti-Stokes photons from a three-level system, we look at a simple experiment of photon coincidence counting measurement, as illustrated in Fig. 1(b). The polarization properties of generated weak fields will be discussed in Sec. IV C.

The averaged two-photon coincidence counting rate is defined by Glauber's theory,

$$R_{cc} = \lim_{T\to\infty} \frac{1}{T} \int_0^T dt_1 \int_0^T dt_2 \langle \Psi | E_1^{(-)}(\tau_1) E_2^{(-)}(\tau_2) E_2^{(+)}(\tau_2) E_1^{(+)}(\tau_1) \times |\Psi\rangle W(\tau_1 - \tau_2). \quad (37)$$

Again, $E_j^{(+)}(\tau_j)$ $(j=1,2)$ are the free-space electromagnetic fields, which are evaluated at detector D_j's coordinates r_j and t_j (i.e., setting $\tau_j = t_j - r_j/c$). $W(\tau_1 - \tau_2)$ is the coincidence window function: $W=1$ for $|\tau_1 - \tau_2| < t_c$; otherwise, $W=0$. For the narrow-band biphoton generation analyzed here, t_c is sufficiently large so that one may set $W=1$. In addition, we have implicitly taken the detectors' efficiencies to be 100% to simplify the discussion. By making use of Eq. (27), the fourth-order field correlation function appearing in Eq. (37) can be written as

$$\begin{aligned} &\langle \Psi | E_1^{(-)}(\tau_1) E_2^{(-)}(\tau_2) E_2^{(+)}(\tau_2) E_1^{(+)}(\tau_1) | \Psi \rangle \\ &= |\langle 0 | E_2^{(+)}(\tau_2) E_1^{(+)}(\tau_1) | \Psi \rangle|^2 \\ &= |A_{12}(\tau_1, \tau_2)|^2, \end{aligned} \quad (38)$$

where the completeness relation is applied. Generally, $A_{12}(\tau)$ is referred to as the two-photon amplitude, or biphoton wave packet.

For simplicity, we assume that there are no filters put before the detectors. From Eq. (38), one thus obtains

$$A_{12}(\tau_1, \tau_2) = \sum_{k_1} \sum_{k_2} E_{k_1} E_{k_2} e^{-i(\omega_1 \tau_1 + \omega_2 \tau_2)} \langle 0 | a_{k_2} a_{k_1} | \Psi \rangle, \quad (39)$$

where the wave vectors are replaced by the corresponding wave numbers. With the help of Eq. (27), the last term on the RHS of Eq. (39) becomes

$$\langle 0 | a_{k_2} a_{k_1} | \Psi \rangle = \sum_{k_s} \sum_{k_{as}} F(k_s, k_{as}) \delta_{k_1 k_{as}} \delta_{k_2 k_s}. \quad (40)$$

Making use of Eq. (28) and converting the summations into the Kronecker δ, one can find

$$A_{12}(\tau_1, \tau_2) = \sum_{k_{as}} \sum_{k_s} A_0 \chi_{as}^{(3)} \delta(\omega_p + \omega_c - \omega_{as} - \omega_s) \Phi(\Delta k L) e^{-i(\omega_1 \tau_1 + \omega_2 \tau_2)}. \quad (41)$$

Here all the slowly varying terms and constants are absorbed into A_0. Converting the sums in Eq. (41) into the usual angular frequency integral and using Eq. (23), the two-photon amplitude [Eq. (41)] can be finally evaluated as

$$\begin{aligned} A_{12}(\tau_+, \tau_-) = A_0 &e^{-i[(\omega_p + \omega_c)\tau_+/2]} e^{-i[(\varpi_{as} - \varpi_s)\tau_-/2]} \\ &\times \int d\delta \chi_{as}^{(3)}(\delta) \mathrm{sinc}\left[\frac{\delta L}{2} \left(\frac{1}{v_{as}} + \frac{1}{c} \right) + \frac{\omega_{21} L}{c} \right] \\ &\times e^{i\delta[L/2(1/v_{as} + 1/c) - \tau_-]}, \end{aligned} \quad (42)$$

where Eqs. (21) and (29) have been used and all the slowly varying phase terms and constants are grouped into A_0. In Eq. (42) we have denoted $\tau_+ = \tau_1 + \tau_2$ and $\tau_- = \tau_1 - \tau_2$. As seen from Eq. (42), the profile of paired Stokes and anti-Stokes photons is determined by both the phase mismatching and the structure of the third-order nonlinear susceptibility. In the following, we will look at the feature of the two-photon interference in two different regions: (1) the effect from the phase mismatching is dominant; and (2) the effect from the third-order nonlinear susceptibility is dominant. Before moving to each case, let us express the third-order nonlinear susceptibility as

$$\chi_{as}^{(3)}(\delta) = \frac{N\hbar |d_{31} d_{32}|^2}{\varepsilon_0 (\Delta_p - i\gamma_{32})} \frac{1}{(\delta - \delta_+ + i\Gamma_+)(\delta - \delta_- + i\Gamma_-)}, \quad (43)$$

where we have used Eqs. (14), (15), and (19). Substituting Eq. (43) into Eq. (42) and keeping only the majority quantities of interest, the biphoton wave packet [Eq. (42)] becomes

$$\begin{aligned} A_{12}(\tau_+, \tau_-) = A_0 &e^{-i[(\omega_p + \omega_c)\tau_+/2]} e^{-i[(\varpi_{as} - \varpi_s)\tau_-/2]} \\ &\times \int d\delta \frac{e^{i\delta[(L/2v_{as}) - \tau_-]}}{(\delta - \delta_+ + i\Gamma_+)(\delta - \delta_- + i\Gamma_-)} \\ &\times \mathrm{sinc}\left(\frac{\delta L}{2v_{as}} + \frac{\omega_{21} L}{c} \right). \end{aligned} \quad (44)$$

All the slowly varying terms and constants are grouped into A_0. The physics of biphoton generation in a three-level system is obvious: the biphoton wave packet (44) [and Eq. (42)] is a convolution between the phase matching and structure of the third-order nonlinear susceptibility. From now on Eq. (44) is the starting point for the following discussions.

1. Phase-mismatching-determined biphoton wave packet

First of all, let us look at the case that the phase mismatching is dominant in determining the profile of the biphoton wave packet. In such a case, the optical depth of the material is sufficiently large so that the anti-Stokes field propagates through the medium with ultrasmall group velocity. To achieve this, it requires a dense medium and the control field needs to be tuned near resonant with its atomic transition. When fully satisfied with these two requirements, the feature of the two-photon amplitude in Eq. (44) is mainly determined by the material dispersion, i.e.,

$$A_1(\tau_+,\tau) = A_1 e^{-i[(\omega_p+\omega_c)\tau_+/2]} e^{-i[(\varpi_{as}-\varpi_s)\tau/2]} \times \int_{-\infty}^{\infty} \mathrm{sinc}\left(\frac{\delta L}{2v_{as}} + \frac{\omega_{21}L}{c}\right) e^{i\delta[(L/2v_{as})-\tau]} d\delta. \tag{45}$$

Again, all the constants have been absorbed into A_1. From now on, we will denote τ_- as τ, as done in Eq. (45). As seen from the above equation, the two-photon amplitude is a Fourier transform of a sinc function. Performing the integral yields

$$A_1(\tau_+,\tau) = A_1 \phi_1(\tau_+)\theta_1(\tau), \tag{46}$$

$$\phi_1(\tau_+) = e^{-i[(\omega_p+\omega_c)\tau_+/2]}, \tag{47}$$

$$\theta_1(\tau) = e^{-i[(\varpi_{as}-\varpi_s)\tau/2]} e^{i(2\omega_{21}v_{as}\tau/c)} \Theta\left(\tau, \frac{L}{v_{as}}\right). \tag{48}$$

In Eq. (48), the step function $\Theta(\tau, L/v_{as})$ is one if $\tau \in (0, L/v_{as})$ and vanishes otherwise; because of $v_{as}/c \ll 1$, the second phase term on the RHS of Eq. (48) is negligible compared with the first one. The physics of Eq. (46) is understood as follows. Because the two-photon state is entangled, it cannot be factorized into a function of τ_1 times a function of τ_2. The term $\phi_1(\tau_+)$ tells that the pair can be randomly created at any time within the medium. If the wave packets of the pump and control beams are rather than a plane wave, this term $\phi_1(\tau_+)$ would become a wave packet with a coherence length of the pump and control. The function $\theta_1(\tau)$ is a step function modified by the beating frequency between paired Stokes and anti-Stokes photons.

By using Eqs. (46) and (48), the two-photon coincidence counting rate [Eq. (37)] now becomes

$$R_{c1}(\tau) = R_1 \Theta\left(\tau, \frac{L}{v_{as}}\right), \tag{49}$$

where R_1 is the grouped constant. The result of Eq. (49) indicates that in the phase-mismatching-dominant case, the two-photon correlation gives the feature of the conventional SPDC. In such a case, the information about the mechanism of generating paired Stokes and anti-Stokes photons inside the material (see Sec. IV B 2) is washed out by the phase-matching condition. In the counterpropagation geometry, if $\mathbf{k}_p + \mathbf{k}_c = 0$ is well satisfied, then $R_{c1}(\tau)$ is a symmetric picture and the feature of photon bunching will be observed.

2. Nonlinear-susceptibility-determined biphoton wave packet

Next, we consider the case that the structure of the third-order nonlinear susceptibility $\chi_{as}^{(3)}(\delta)$ mainly determines the profile of the biphoton wave packet. To obtain such a case, it requires that the optical depth is not quite so large that the spectral width of the biphoton wave packet is mainly dependent on the structure of $\chi^{(3)}$, not upon the effects from the first-order optical response χ. The two-photon amplitude in Eq. (44) now turns out to be the Fourier transform of $\chi_{as}^{(3)}(\delta)$,

$$A_2(\tau_+,\tau) = A_2 e^{-i[(\omega_p+\omega_c)\tau_+/2]} e^{-i[(\varpi_{as}-\varpi_s)\tau/2]} \times \int \frac{e^{-i\delta\tau} d\delta}{(\delta-\delta_+ + i\Gamma_+)(\delta-\delta_- + i\Gamma_-)}. \tag{50}$$

Again, A_2 has absorbed all the constants and slowly varying terms. By calculating the residues in Eq. (50), it gives

$$A_2(\tau_+,\tau) = A_2 \phi_2(\tau_+)\theta_2(\tau), \tag{51}$$

$$\phi_2(\tau_+) = e^{-i[(\omega_p+\omega_c)\tau_+/2]}, \tag{52}$$

$$\theta_2(\tau) = e^{i[(\omega_{21}-\Delta_p)\tau/2]}(e^{-i(\Omega_e\tau/2)} e^{-\Gamma_+\tau} - e^{i(\Omega_e\tau/2)} e^{-\Gamma_-\tau}). \tag{53}$$

The physics behind $\theta_2(\tau)$ is that in the two-photon amplitude, there is a destructive interference between two types of FWMs concealed in $\chi_{as}^{(3)}(\delta)$, as discussed in Sec. II. The first term in the brackets on the RHS of Eq. (53) represents the two-photon amplitude between paired anti-Stokes (central frequency at $\varpi_{as} = \omega_{31} - \delta_-$) and Stokes (central frequency at $\omega_s = \omega_{32} - \Delta_p - \delta_+$) with the spectral width Γ_+; while the second term is the two-photon amplitude between paired anti-Stokes (peaked at $\varpi_{as} = \omega_{31} - \delta_+$) and Stokes (peaked at $\varpi_s = \omega_{32} - \Delta_p - \delta_-$) with spectral width Γ_-. The sum of these two two-photon amplitudes is manifested by a slowly oscillating phase term. To further see the interference between two types of FWMs, let us examine the two-photon coincidence counting rate.

By substituting Eqs. (51) and (53) into Eq. (37), it is easy to find

$$R_{c2}(\tau) = R_2[e^{-2\Gamma_+\tau} + e^{-2\Gamma_-\tau} - 2\cos(\Omega_e\tau)e^{-(\Gamma_+ + \Gamma_-)\tau}], \tag{54}$$

where R_2 is a constant. Now the physics is obvious: the first term in Eq. (54) corresponds to the correlation between paired anti-Stokes (central frequency at $\varpi_{as} = \omega_{31} - \delta_-$) and Stokes (central frequency at $\omega_s = \omega_{32} - \Delta_p - \delta_+$), the second one to the correlation between paired anti-Stokes (peaked at $\varpi_{as} = \omega_{31} - \delta_+$) and Stokes (peaked at $\varpi_s = \omega_{32} - \Delta_p - \delta_-$), and the third one appears as a destructive interference between two previous terms. The two-photon interference pattern is a damped Rabi oscillation and the oscillation frequency is equal to the effective Rabi frequency Ω_e. The damping rate is determined by the resonant linewidths in the doublets. At $\tau = 0$, the function R_{c2} vanishes, exhibiting the photon antibunching-like effect. As $\tau \to \infty$, R_{c2} also approaches to zero. When the control field is near resonant with its transition

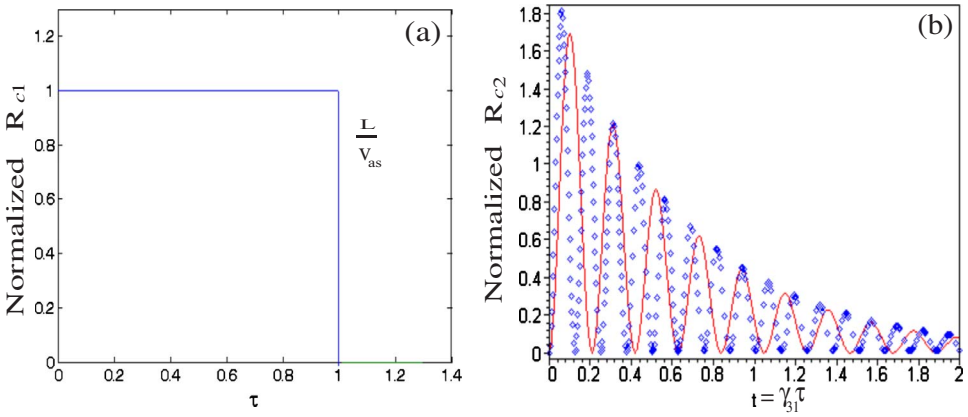

FIG. 3. (Color online) The normalized two-photon coincidence counting rate in two different regimes, where the paired Stokes-anti-Stokes wave packet is determined by (a) the phase matching and (b) the structure of doublet resonances shown in the third-order nonlinearity. In (b), the red solid line represents the control field resonant with its transition and the blue point line is the opposite case.

channel, the spectral widths of two types of FWMs are the same, i.e., $\Gamma_+=\Gamma_-=\frac{\gamma_{31}+\gamma_{21}}{2}$. Under such a situation, Eq. (54) reduces to a simple form

$$R_{c2}(\tau) = R_2[1-\cos(\Omega_e\tau)]e^{-(\gamma_{31}+\gamma_{21})\tau}. \tag{55}$$

If $k_p=k_c$, $R_{c2}(\tau)$ is a symmetric distribution about $\tau=0$, because spontaneously emitted paired photons can trigger both detectors D_1 and D_2.

Comparing with the case discussed in the above section, the main difference comes from that whose effect plays a key role in determining the properties of the biphoton wave packet between the linear response and the third-order nonlinearity. If the effects (dispersion and transmission) from the first-order susceptibility are dominant, then the information about the two types of FWM processes are hidden by the longer timing due to the dispersion. However, in the case that spectral widths of biphotons are determined by the resonance linewidths instead of the phase-matching condition, the two-photon interference pattern displays the structure of the third-order optical response.

In Fig. 3, the patterns of the two-photon coincidence counting rate are simulated for the cases discussed above. Figure 3(a) represents the situation that the phase mismatching determines the spectral width of the biphoton wave packet. $R_{c1}(\tau)$ gives a feature of Heaviside function. In Fig. 3(b), the two-photon wave packet is determined by the third-order nonlinear susceptibility. The (red) solid line describes that the control field is resonant with its transition channel. The (blue) point line assumes that the control detuning is equal to its Rabi frequency. The two-photon coincidences $R_{c2}(\tau)$ are a damped Rabi oscillation with oscillation period $2\pi/\Omega_e$ and decay rate $\gamma_{31}+\gamma_{21}$. At $\tau=0$, R_{c2} goes to zero, indicating a destructive interference occurring between two types of FWM processes in such a case. If $\mathbf{k}_p+\mathbf{k}_c=0$, symmetric features about $\tau=0$ are expected to be observed. Comparing Fig. 3(a) with Fig. 3(b), one difference is that around $\tau=0$, Fig. 3(a) gives the photon bunching effect while Fig. 3(b) exhibits the photon antibunching effect.

C. Polarization-entanglement generation

As mentioned in Sec. II, the scheme can be used to generate polarization-entangled Stokes and anti-Stokes photons, such as the degenerate type-II SPDC. In this section, we focus on the polarization-entangled state for different cases. As shown in Fig. 4, two counterpropagating pump and control lasers are circularly polarized with $\sigma^+-\sigma^-$ configuration and applied to a three-state system. Polarization-entangled biphotons are spontaneously emitted into the backward geometry. Since $k_p\neq k_c$, the detection system is better to be operated in the collinear-propagation experimental setup. (The right-angle geometry still works in this case except that the collection efficiency is decreased, because of the directionality of the input lasers.) Following the analysis in Sec. IV B, there are two different cases to achieve polarization-entangled photon pairs. One case is that the biphoton wave packet is mainly determined by the phase-matching condition (see Sec. IV B 1). As the experiment operates in this region, the intrinsic mechanism of biphoton generation is washed out by the phase matching. Satisfying the requirement of $\omega_{21}=-\Delta_p-\Delta_c$, one can obtain the polarization-entangled Stokes and anti-Stokes state as in the degenerate type-II SPDC. The normalized state reads

$$|\Psi^+\rangle = \frac{1}{\sqrt{2}}(|\sigma^-\rangle_s|\sigma^+\rangle_{as} + |\sigma^+\rangle_s|\sigma^-\rangle_{as}), \tag{56}$$

where the left- and right-circularly polarized single-photon states are donated as $|\sigma^-\rangle$ and $|\sigma^+\rangle$, respectively. Equation (56) is one member out of a set of four states known as Bell states.

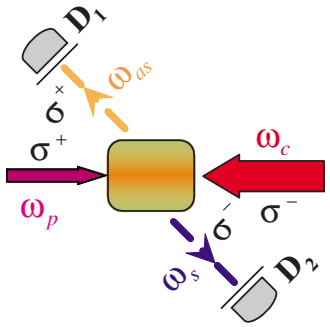

FIG. 4. (Color online) Polarization-entangled Stokes-anti-Stokes generation in a three-state scheme. Two counterpropagating pump and control beams are circularly polarized with $\sigma^+-\sigma^-$ configuration.

The second case is that the structure of the biphoton wave packet is almost controlled by the third-order nonlinearity, i.e., two types of FWM processes will be revealed in the coincidence counting measurement, as discussed in Sec. IV B 2. To obtain the polarization entanglement in such a case, there are two opportunities as mentioned in Sec. II; $\omega_{21}=-\Delta_p\pm\Omega_e$. Alternatively, one can choose one FWM to create the polarization-entangled state and leave the other nonpolarization entangled because of the energy difference. Suppose that the condition $\omega_{21}=-\Delta_p+\Omega_e$ is satisfied. The output state at the surfaces then becomes

$$|\Psi^+(\tau)\rangle = \frac{1}{2}e^{-i(\Omega_e\pi/2)}e^{-\Gamma_+\tau}(|\sigma^-\rangle_s|\sigma^+\rangle_{as} + |\sigma^+\rangle_s|\sigma^-\rangle_{as}) - \frac{1}{\sqrt{2}}e^{i(\Omega_e\pi/2)}e^{-\Gamma_-\tau}|1\rangle_{as}|1\rangle_s, \quad (57)$$

where $|1\rangle_{as}|1\rangle_s$ represents the nonpolarization-entangled photon pairs in which the anti-Stokes is peaked at $\omega_{31}-\delta_-$ and the Stokes is peaked at $\omega_{31}-\delta_--2\Omega_e$. The nonpolarization-entangled paired photons will increase the background coincidences and decrease the visibility in the application of the optical test of local realistic theories and Bell's theorem. Hence, to fulfill the testing, filtering one type of FWM process is necessary to eliminate the nonpolarization-entangled part and enhance the visibility.

As shown in the above, the efficiency of paired Stokes and anti-Stokes photons is proportional to the third-order nonlinearity $\chi^{(3)}$. To enhance the efficiency of polarization-entangled photon pairs, it is desirable to increase the intensity of the control beam and/or decrease the pump detuning. Since these entangled photons have narrow bandwidth, long coherence time and coherence length, they are useful for long distance quantum communication by using EIT as quantum memory to manipulate the nonclassical light [27].

V. SUMMARY

In this paper, we have extensively studied the optical properties of the paired Stokes and anti-Stokes generation in a three-level double-Λ system in the large pump-detuning case. To catch the physics instead of the complicated analysis, the Doppler broadening and quantum Langevin noise are not taken into account. The third-order nonlinear susceptibility shows that there are two types of FWMs happening in the system. Working in the counterpropagation geometry, we find that in general, the biphoton wave packet is a convolution of the longitudinal detuning function and the third-order nonlinear susceptibility. Therefore, the two-photon amplitude is divided into two regimes according to the dominant effect from either the phase matching or the doublet resonances shown in $\chi^{(3)}$. When the phase matching determines the properties of the biphoton wave packet, the coincidence counting rate gives the pattern as the conventional SPDC. The detailed information of two types of biphoton generation is washed out by the phase matching because of its longer timing window. If the spectral width of the biphoton wave packet is mainly characterized by the resonant linewidths of the doublet, the two-photon joint detection probability reveals two FWMs occurring in the medium. The two-photon correlation pattern gives a damped Rabi oscillation due to the destructive interference between two types of FWM processes. The oscillation frequency is equal to the effective Rabi frequency Ω_e, and the damping rate is determined by the resonant linewidths Γ_+ and Γ_-. The theory agrees with the experiment in such a case. If $\mathbf{k}_p+\mathbf{k}_c=0$ is satisfied, the pattern of the two-photon temporal correlation is a symmetric distribution. One can choose the right-angle geometry to eliminate the Rayleigh scattering of the pump and control beams in such a situation. If $\mathbf{k}_p+\mathbf{k}_c\neq 0$, a collinear-propagation scheme is better to collect paired Stokes and anti-Stokes photons.

We have also examined generating the polarization-entangled state in two situations in a three-state system. If the phase matching controls the biphoton wave packet, the state takes the same form as the conventional degenerate type-II SPDC case. If the doublet resonances play the dominant role in determining the two-photon amplitude, the output state at the material surfaces is a mixture of polarization-entangled part plus nonpolarization-entangled part. This latter case will increase the background coincidences in testing the realistic theories and Bell's theorem, and as a result decrease the visibility. To fulfill the testing, filtering one type of FWM process is necessary to enhance the visibility.

ACKNOWLEDGMENTS

We wish to thank Eun Oh for fruitful discussions. J.-M.W. and M.H.R. were supported in part by the U.S. Army Research Office under MURI Grant No. W911NF-05-1-0197. S.D. acknowledges financial support from the Defense Advanced Research Projects Agency, the U.S. Air Force Office of Scientific Research, and the U.S. Army Research Office.

[1] M. A. Neilson and I. L. Chuang, *Quantum Computation and Quantum Information* (Cambridge University Press, Cambridge, England, 2000).

[2] A. Einstein, B. Podolsky, and N. Rosen, Phys. Rev. **47**, 777 (1935).

[3] E. Schrödinger, Naturwiss. **23**, 807 (1935); **23**, 823 (1935); **23**, 844 (1935) [translation in *Quantum Theory of Measurement*, edited by J. A. Wheeler and W. H. Zurek (Princeton University Press, Princeton, 1983)].

[4] D. Bohm, *Quantum Theory* (Prentice-Hall, Englewood Cliffs, NJ, 1951).

[5] D. M. Greenberger, M. Horne, and A. Zeilinger, in *Bell's Theorem, Quantum Theory, and Conceptions of the Universe*, edited by M. Kafatos (Kluwer, Dordrecht, 1989), p. 73.

[6] D. N. Klyshko, Sov. Phys. Usp. **31**, 74 (1988); Usp. Fiz. Nauk **154**, 133 (1988).

[7] A. N. Boto, P. Kok, D. S. Abrams, S. L. Braunstein, C. P. Williams, and J. P. Dowling, Phys. Rev. Lett. **85**, 2733 (2000); M. D'Angelo, M. V. Chekhova, and Y. Shih, *ibid.* **87**, 013602 (2001).
[8] A. Migdall, R. Datla, A. V. Segienko, J. S. Orszak, and Y.-H. Shih, Appl. Opt. **37**, 3455 (1998).
[9] M. H. Rubin, D. N. Klyshko, Y.-H. Shih, and A. V. Sergienko, Phys. Rev. A **50**, 5122 (1994); D. N. Klyshko, *Photons and Nonlinear Optics* (Gordon and Breach Science, New York, 1988).
[10] M. H. Rubin, Phys. Rev. A **54**, 5349 (1996); Y.-H. Shih, Rep. Prog. Phys. **66**, 1009 (2003).
[11] S. E. Harris, Phys. Today **50**(7), 36 (1997).
[12] D. A. Braje, V. Balić, S. Goda, G. Y. Yin, and S. E. Harris, Phys. Rev. Lett. **93**, 183601 (2004).
[13] V. Balić, D. A. Braje, P. Kolchin, G. Y. Yin, and S. E. Harris, Phys. Rev. Lett. **94**, 183601 (2005).
[14] P. Kolchin, S. Du, C. Belthangady, G. Y. Yin, and S. E. Harris, Phys. Rev. Lett. **97**, 113602 (2006).
[15] S. Du, J.-M. Wen, M. H. Rubin, and G. Y. Yin, Phys. Rev. Lett. **98**, 053601 (2007).
[16] J.-M. Wen and M. H. Rubin, Phys. Rev. A **74**, 023808 (2006); **74**, 023809 (2006).
[17] J.-M. Wen, S. Du, and M. H. Rubin, Phys. Rev. A **75**, 033809 (2007).
[18] P. Kolchin, Phys. Rev. A **75**, 033814 (2007).
[19] J.-M. Wen, S. Du, and M. H. Rubin, Phys. Rev. Lett. (to be published).
[20] R. W. Boyd, *Nonlinear Optics* (Academic Press, San Diego, California, 1992).
[21] S. Du, E. Oh, J.-M. Wen, and M. H. Rubin, Phys. Rev. A **76**, 013803 (2007).
[22] J.-M. Wen, P. Xu, M. H. Rubin, and Y.-H. Shih, Phys. Rev. A (to be published).
[23] J.-M. Wen, M. H. Rubin, and S. Du (unpublished).
[24] J. S. Bell, Physics (Long Island City, N.Y.) **1**, 195 (1964); J. S. Bell, *Speakable and Unspeakable in Quantum Mechanics* (Cambridge University Press, New York, 1989).
[25] N. Gisin, G. Ribordy, W. Tittel, and H. Zbinden, Rev. Mod. Phys. **74**, 145 (2002).
[26] Y. R. Shen, *The Principles of Nonlinear Optics* (Wiley-Interscience, New York, 1984).
[27] J.-M. Wen and M. H. Rubin, Phys. Rev. A **70**, 063806 (2004).